*sustainability*

MDPI

*Article*

# Multi-Scenario Simulation of Land Use/Cover Change and Terrestrial Ecosystem Carbon Reserve Response in Liaoning Province, China

**Hanlong Gu, Jiabin Li and Shuai Wang ***

College of Land and Environment, Shenyang Agriculture University, Shenyang 110866, China; 2015500018@syau.edu.cn (H.G.); 2022240547@stu.syau.edu.cn (J.L.)
* Correspondence: shuaiwang666@syau.edu.cn

**Abstract:** Land use/cover change (LUCC) can either enhance the areal carbon reserve capacity or exacerbate carbon emission issues, thereby significantly influencing global climate change. Comprehending the impact of LUCC on regional carbon reserve variation holds great significance for regional ecosystem preservation and socioeconomic sustainable development. This study focuses on Liaoning Province, leveraging land use remote sensing data from three periods from 2000 to 2020, natural environmental data and socioeconomic data in conjunction with the Integrated Valuation of Environmental Services and Trade-offs (InVEST) model, and patch-generating land use simulation (PLUS) models. It analyzes the interactive relationship between LUCC and carbon reserves in Liaoning Province between 2000 and 2020 and forecasts the trajectory of carbon reserve changes in Liaoning Province under various scenarios: business as usual, urban development, cropland protection, and ecological protection, all based on LUCC simulations. The findings indicate the following: (1) Over the study period, Liaoning Province experienced significant LUCC characterized primarily by the transformation of farmland to built-up land. Carbon reserves initially declined and later increased due to LUCC changes, resulting in a cumulative increase of 30.52 Tg C. The spatial distribution of carbon reserves was influenced by LUCC, displaying a pattern of spatial aggregation, with higher values in the east and lower values in the west. (2) Across the four simulation scenarios, the spatial pattern of carbon reserves in Liaoning Province continued to exhibit the characteristic spatial aggregation of higher values in the east and lower values in the west. Under the urban development scenario, carbon reserves decreased by 34.56 Tg C tons, representing a 2.45% decrease compared to 2020. Conversely, under the business-as-usual, cultivated land protection, and ecological protection scenarios, carbon reserves displayed a growing tendency, reaching 1449.35 Tg C, 1450.39 Tg C, and 1471.80 Tg C, respectively, with changes of 0.09%, 0.16% and 1.63% compared to 2020. The substantial increase in carbon reserves under the ecological protection scenario primarily stemmed from the significant expansion of woodland and other ecological land areas. In light of these findings, Liaoning Province may consider laying down and strictly executing spatial policies for ecological protection in future land projecting. The PLUS model and InVEST model can help curb the uncontrolled expansion of built-up land, facilitate the increment of ecological land areas, and with effect augment carbon reserves, thereby ensuring the achievement of the "double carbon" target of carbon peak and carbon neutralization.

**Keywords:** LUCC; carbon reserve; PLUS model; InVEST model; scenario simulation; Liaoning Province



**Citation:** Gu, H.; Li, J.; Wang, S. Multi-Scenario Simulation of Land Use/Cover Change and Terrestrial Ecosystem Carbon Reserve Response in Liaoning Province, China. *Sustainability* **2024**, *16*, 8244. https://doi.org/10.3390/su16188244

Academic Editor: Anna De Marco

Received: 29 August 2024
Revised: 18 September 2024
Accepted: 20 September 2024
Published: 22 September 2024



## 1. Introduction

Land use/cover change (LUCC) stands as a pivotal driver of worldwide environmental challenges, with its influence on the carbon cycle of terrestrial ecological systems gaining significance within climate change exploration [1]. Carbon reserves in terrestrial ecosystems are an essential facet in the worldwide carbon cycle, atmospheric carbon dioxide awareness,

and broader climate change dynamics [2]. LUCC can alter terrestrial carbon stocks by reshaping the ecosystem structure and function [3]. The yearly net carbon soak-up of terrestrial ecological systems extends between 2.0 Pg and 3.4 Pg. Globally, LUCC-induced carbon emissions in 2020 amounted to 0.9 ± 0.7 Gt C [4]. LUCC contributes approximately one-third of the carbon releases contributed to anthropo-operations since the industrial revolution, ranking as the second-largest carbon discharge source following fossil fuels. Both the United Nations Framework Convention on Climate Change (UNFCCC) and the Kyoto Protocol advocate for measures to mitigate carbon releases and underscore the importance of carbon reserves in terrestrial ecosystems, garnering widespread agreement among governments and scholars [5]. Moreover, reports by the Intergovernmental Panel on Climate Change (IPCC) underscore LUCC's significant facet in bolstering carbon reserves within terrestrial ecosystems [6]. Hence, intensifying carbon reserve efforts and curbing carbon emissions enjoy global consensus, prompting collaborative actions worldwide to address the adverse impacts of climate variation [7].

As the world's second-largest economy, China has emerged as the largest greenhouse gas emitter globally, having contributed30.7% of global carbon dioxide emissions by 2020 [8]. Additionally, China, being the largest developing country, has witnessed unprecedented urbanization growth in recent decades, with the urbanization rate reaching 64.7% in 2021. This speedy urbanization progression has prominently bolstered economic advancement and living standards but has profoundly impacted land use patterns [9]. Consequently, extensive urban expansion has led to the degradation of vast stretches of fertile arable land and ecological areas, giving rise to a marked descend in China's overall land ecosystem carbon storage capacity [10]. China, recognized for its potential to play a leading role on the global stage, has actively assumed responsibility for global carbon reduction endeavors, outlining clear objectives in national policies to combat climate change. These objectives include striving to reduce anthropogenic carbon emissions, heightening ecological system carbon stocks, achieving the 2030 carbon peak target, and attaining carbon neutrality by 2060 [11].

Land use models have become irreplaceable technical tools for studying the processes and mechanisms of land use and cover change (LUCC) and their ecological influences. Various existing land use models, such as the CA-Markov model, the CLUE-S model, and the FLUS model, have been extensively utilized to depict the spatiotemporal types of LUCC [12]. For instance, Sun et al. [13] adopted the CA-Markov model to plumb the effect of land use on the sight pattern of wetlands in different periods in the Huang he River basin. Hamad et al. [14] applied the CA-Markov model to analyze and forecast the spatiotemporal distribution of land use/cover change in the pivotal protected zone (HSCZ) of Iraqi Kurdistan. Lin et al. [15] constructed the ANN-CA model in the MATLAB (R2018a) platform to simulate the Tarim River around the main city of Korla, and concluded that the implementation of an ecological water transfer policy has a significant effect on the LULC changes in arid and semi-arid areas. Additionally, Cong et al. [16] employed the CLUE-S model to analyze land use variations under multiple scenarios in the South Four Lake basin, while Gu et al. [17] based their simulation analysis on the CLUE-S model to project land use spatial patterns in Faku County under various future conditions. Furthermore, Liu et al. [18] employed the FLUS model to analyze land use changes in Xiangyun County by 2025, and Tang et al. [19] employed the FLUS model to project the spatiotemporal spread of land use in the Qingyi River basin until 2035. However, these models have boundedness in discerning the prospective driving forces of LUCC and cannot dynamically identify multiple land type plaques, especially the succession of natural land type plaques [20]. In contrast, the patch-generating land use simulation (PLUS) model, based on the rule mining framework of the Land Extension Analysis Strategy (LEAS) and the cellular automata (CA) module based on multi-type stochastic patch seeding (CARS), aims to comprehensively explore the various factors that affect land use change. The cellular automata (CA) model is known to be able to roughly simulate spatial changes in complex systems in terms of simulating land use changes. The PLUS model can not only simulate all types of land

use patch-level changes, but also has a high simulation accuracy and a wide range of applicability, which effectively solves the problem of accuracy in the simulation of large-scale land use data, better reflects the impacts of the LUCC on ecosystem services in the future, and is more suitable for accurately modeling the potential development needs of LUCC under different scenarios in the future [21].

Existing methods for appraising carbon reserves in terrestrial ecological systems primarily embody on-the-spot investigation, remote sensing inversion, and model prediction. Field sampling and carbon density measurement with specialized equipment are suitable for small-scale investigations of carbon reserves but are time-consuming and destructive [22]. Remote sensing inversion estimates forest biomass by analyzing the spectral characteristics of vegetation reflection, which is easy to obtain and cost-effective but lacks precision and may introduce errors [23]. Model-based approaches simulate carbon stocks using remote sensing imagery, employing bookkeeping or InVEST models to illustrate the relationship between carbon stock distribution and human activities. Among these methods, the Integrated Valuation of Ecosystem Services and Tradeoffs (InVEST) model is preponderant in operational simplicity, parameter flexibility, and accuracy, enabling visualization of the spatiotemporal distribution of carbon reserves [24]. Currently, numerous scholars applied the InVEST model to appraise carbon reserve levels in various zones from dissimilar viewpoints [25]. The InVEST model can also calculate current and future carbon stocks and losses in a region and has therefore been widely used in recent carbon stock estimation studies. For instance, Yang et al. [26] applied the InVEST model to estimate carbon storage in the Yellow River Basin. Wei et al. [27] employed the InVEST model to appraise variations in carbon reserves in the Loess Plateau, exploring the contributions of returning cropland to woodland and grasslands and the establishment of preserved regions for zonal carbon sequestration.

Given the vastness of China and its multifarious land patterns [28], Liaoning Province stands out as one of the important old industrial bases in the country, boasting thriving heavy and raw material industries that significantly contribute to the national economy. However, industrialization's advancement has also exacerbated eco-environmental challenges, such as eco-environmental degradation and land resource wastage. Despite implementing various ecological protection projects, the local ecosystem remains fragile, grappling with issues like degraded forest structure, land desertification, and high carbon emissions levels. Hence, there is an urgent need to address sustainable development concerns regarding land use and ecological system carbon reserves [29]. As of now, Liaoning Province lacks simulation studies on future development scenarios and carbon reserves, hindering scientific regional land use planning. To address this gap, this paper focuses on Liaoning Province, which is a heavy industrial base and high energy-consuming province in China and is a key area for realizing the dual carbon target, aiming to establish various development scenarios using a combination of InVEST and PLUS models. Through systematic simulation and analysis of land use variations and carbon reserves from 2000 to 2030, the study seeks to enhance regional ecosystem carbon reserves in Liaoning Province and offer crucial theoretical and practical insights for the land spatial patterns of the majorization in line with the "double carbon" objective. The preponderant orientations of this paper are as follows: (1) assessing variations in land use patterns over time using the PLUS model and investigating potential future development scenarios for sustainable land use planning; (2) evaluating changes in carbon reserves within the regional ecosystem from 2000 to 2030 using the InVEST model; (3) providing practical recommendations for enhancing regional ecosystem carbon reserves based on simulation results and analyzing current eco-environmental challenges faced by Liaoning Province due to industrialization. Furthermore, it actively aligns with the national agenda of low-carbon, green, and sustainable development amidst the backdrop of carbon neutrality, offering theoretical underpinnings and scientific decision-making references for sustainable land resource utilization, ecological environment conservancy, and strategic sustainable development [30].

## 2. Materials and Methods

### *2.1. Study Area*

Liaoning Province is situated in the northeast of China (118°53′ E–125°46′ E, 38°43′ N–43°26′ N), bordering the Yellow Sea and Bohai Sea to the south, and the Yalu River to the southeast, with North Korea across the river. It spans approximately 146,100 square kilometers. The region's geomorphological features are characterized by six mountains and one body of water; generally, the topography is higher in the north and lower in the south, slanting from land to sea, with mountains and hills flanking the east and west sides, tilting toward the focal plains [31], as shown in Figure 1. Liaoning Province keeps a temperate monsoon climate, with a yearly mean temperature transforming from 7 °C to 11 °C [32]. Dominated by cultivated land, it serves as a crucial national grain production area. In 2022, Liaoning Province's GDP reached CNY 289.751 billion, marking a 2.1% increase compared to the previous year. Over the past few years, rapid urbanization has eventuated significant dilation of urban impervious land in Liaoning Province, with an average yearly augment speed of 51% over the past five years—ranking highest among the three eastern provinces and surpassing the national average [33]. In this context, clarifying the interactive relevance between land use patterns and carbon reserve levels in Liaoning Province, as well as forecasting variations in carbon reserves under dissimilar regional advancement scenarios in the future, holds significant practical importance [34]. The types of land use in Liaoning Province are diverse, primarily including cultivated land, forestland, and grassland, with widespread suitability for resource utilization and great production potential. Such insights can inform future development paths and land use strategies, effectively contributing to carbon reduction goals and increased carbon sequestration.

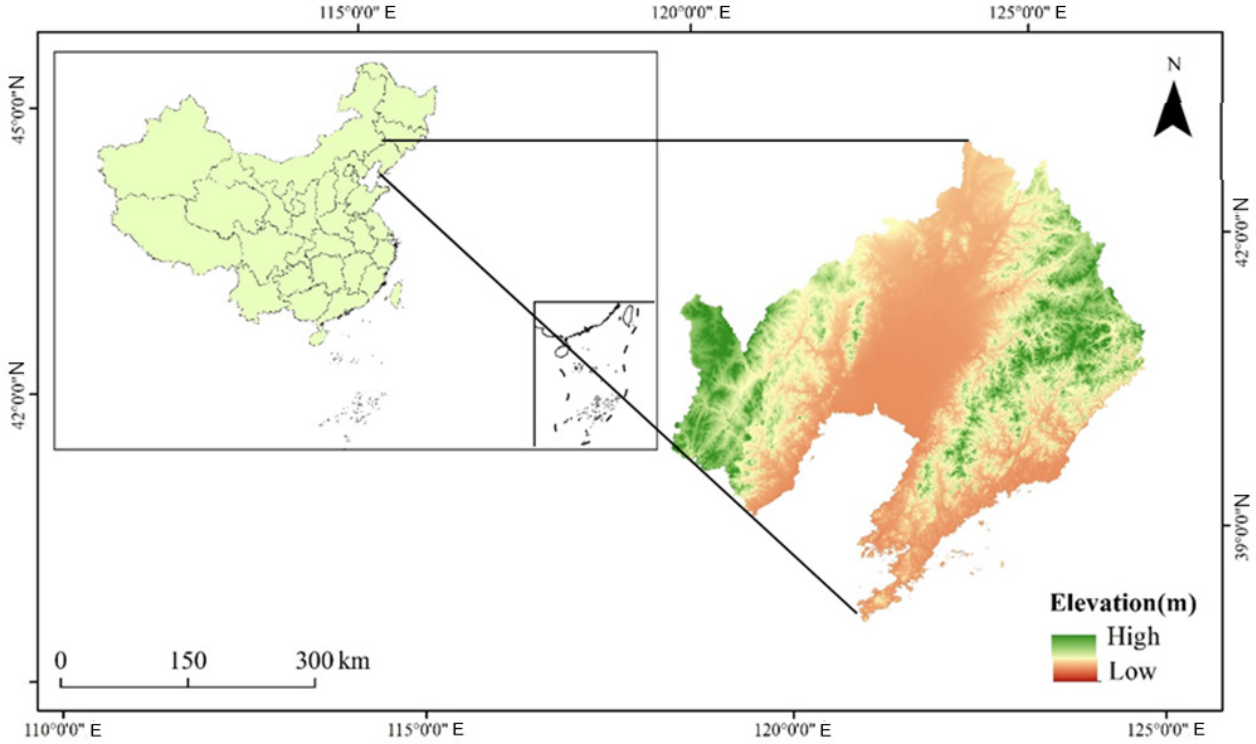


**Figure 1.** Location of the study area.

### *2.2. Data Sources*

#### 2.2.1. Driving Factors

The datasets utilized in this study encompass various categories: land use data, natural factors, and socioeconomic factors (Table 1). A detailed description of each dataset is provided below: (1) Land use data for the years 2000, 2010, and 2020 were attained

from the Chinese Academy of Sciences Resource and Environment Science Data Center [4]. These datasets were separated out into six types: arable land, woodland, grassland, water, impervious land, and bare land [35]. (2) Natural Environmental Factors: This category includes soil pattern data for 2018 obtained from the Chinese Academy of Sciences Resource and Environment Science Data Center, annual average temperature data for 2022 sourced from the China Meteorological Administration, Digital Elevation Model (DEM) data for 2022 collected from the Geospatial Data Cloud, and slope data derived from the DEM through processing in ArcGIS 10.7 software [36]. (3) Socioeconomic Factors: Socioeconomic data for the year 2022, including population density and gross domestic product (GDP), were sourced from the Chinese Academy of Sciences Resource and Environment Science Data Center [37]. These data calculated the yearly average population density and GDP. Transportation data for 2022, comprising road, rail, waterway, and distance to township information, were gathered from OpenStreetMap and processed into a distance grid using the Euclidean distance method [38]. All datasets were projected onto the WGS_1984_UTM_Zone_50N frame of axes [39].

**Table 1.** Details of driving factor data.

| Data Type | Designation | Year | Resolution | Sources |
|---|---|---|---|---|
| Land use data | Land use | 2000, 2010, 2020 | 30 m × 30 m | Resource and Environmental Science and Data Center of the Chinese Academy of Sciences (https://www.resdc.cn/) (accessed on 25 June 2023) |
| Natural environmental factors | Soil type | 2022 | 1000 m × 1000 m | https://www.resdc.cn/ (accessed on 25 June 2023) |
| | Temperature | 2022 | 1000 m × 1000 m | China Meterological Administration (https://data.cma.cn/) (accessed on 13 July 2023) |
| | DEM | 2022 | 30 m × 30 m | Geospatial Data Cloud (https://www.gscloud.cn/home) (accessed on 13 July 2023) |
| | Slope | 2022 | 30 m × 30 m | https://www.resdc.cn/ (accessed on 10 July 2023) |
| Socioeconomic factors | Population | 20 22 | 100 m × 100 m | https://www.resdc.cn/ (accessed on 10 July 2023) |
| | GDP | 202 2 | 1000 m × 1000 m | https://www.resdc.cn/ (accessed on 10 July 2023) |
| | Adjacent to the railway station | 20 22 | 100 m × 100 m | OSM (https://www.openstreetmap.org/) (accessed on 15 July 2023) Using DEM through Euclidean distance calculation in ArcGIS |
| | Adjacent to the highway | 20 22 | | |
| | Adjacent river water body | 20 22 | | |
| | Adjacent towns | 20 22 | | |

#### 2.2.2. Carbon Density Data

LUCC type carbon density data are given in Table 2. Carbon density data are an important parameter for the accurate evaluation of carbon reserves in the InVEST model, and the carbon pool data mainly refer to public datasets and previous literature, and in order to minimize the error, the carbon density data obtained from field sampling of various types of land in Liaoning Province and adjacent study areas are selected as much as possible [40]. LUCC Type Carbon Density Data: LUCC type carbon density data are categorized into four types: aboveground biomass carbon density, belowground biomass carbon density, soil organic matter carbon density, and dead organic matter carbon density.

**Table 2.** Carbon density of each LUCC type (t/hm$^2$).

| LUCC Type | Aboveground | Belowground | Soil Organic | Dead Organic |
|---|---|---|---|---|
| Cropland | 4.75 | 0 | 33.51 | 0 |
| Forest | 49.6 | 24.97 | 128.67 | 1.99 |
| Grassland | 24.38 | 19.59 | 52.29 | 22.74 |
| Water | 2.45 | 0.62 | 80.11 | 0.1 |
| Built-up land | 4.33 | 2.17 | 6.37 | 0.58 |
| Bare land | 0 | 0 | 0 | 0 |

### *2.3. Research Framework and Study Methods*

#### 2.3.1. Research Framework

The research framework of this paper is divided into two parts: the PLUS model was adopted to compute LUCC and the InVEST model was applied to calculate and assess carbon reserves, as shown in Figure 2. Specifically, the PLUS model was adopted to forecast the spatial–temporal pattern of land use under four scenarios in 2030, restricted by the driving factors of population density, GDP, DEM and so on, with the land use data of Liaoning Province from 2000, 2010, and 2020; the InVEST model was employed to receive the spatial–temporal changes of carbon reserves and their features, resulting from LUCC during the period from 2000 to 2030.

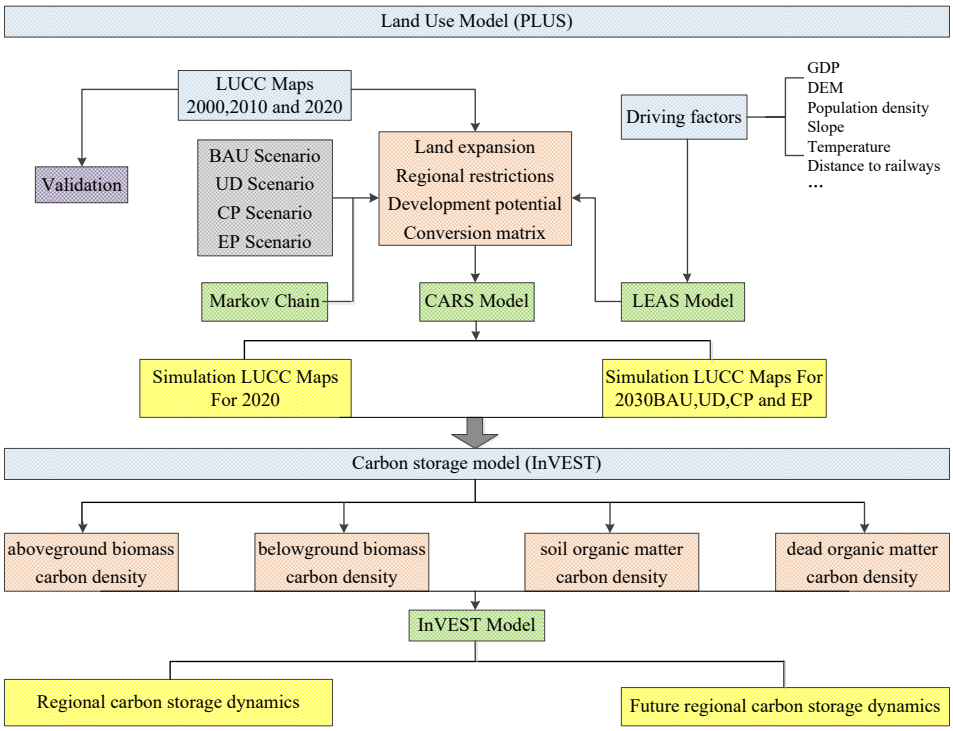


**Figure 2.** Research framework for spatial–temporal analysis.

#### 2.3.2. LUCC Dynamic Analysis

In this study, a LUCC transfer matrix is utilized to analyze LUCC changes. The spatial location and LUCC transfer matrix of LUCC types are generated using the Field Calculator in ArcGIS 10.7 and Origin 2022. The transfer matrix is depicted as below [41]:

$$A = \begin{bmatrix} A_{11} & \cdots & A_{1n} \\ \vdots & \ddots & \vdots \\ A_{n1} & \cdots & A_{nn} \end{bmatrix} \quad (1)$$

where $A$ indicates the LUCC transfer matrix from year to year; the $A_{ij}$ of the matrix indicates the percentage or plenary domain of the transfer from type $i$ to type $j$.

2.3.3. LUCC Simulation Using the PLUS Model

The land expansion analysis strategy (LEAS) element of the PLUS model is employed, along with relevant elements, to tally up the development odds of dissimilar land use patterns. Subsequently, future land use patterns are imitated by applying the CA-Markov model.

1. The Markov model is utilized to forecast land utilization rates.

$$D_{t2} = D_{t1} \times A^{\frac{t_2 - t_1}{a}} \quad (2)$$

$D_{t2}$ represents the LUCC demand at time $t_2$; $D_{t1}$ represents the LUCC status at $t_1$; $A$ denotes the LUCC transfer matrix between years; and $a$ represents the distinct between the start year and the end year of $A$.

2. LUCC Simulation and Validation for Future Scenarios

Random forest classification, a classifier based on integrated decision trees, is utilized for LUCC simulation and verification in future scenarios. This approach involves taking random samples from the LUCC expansion graph, calculating the relationship between expansion and the driver of each LUCC type, and obtaining the expansion probability of each LUCC type at different image pixels. The equation for this process is as below [21]:

$$A_{i,j}^{d}(x) = \frac{\sum_{n=1}^{M} I(h_n(x) = d)}{M} \quad (3)$$

In the expression, the $d$ value can be 0 or 1, where 1 indicates the transformation of other land patterns to land pattern $j$, and 0 denotes any other land use transformation that does not embodying land pattern $j$; $I(\bullet)$ is the pointer ability of the decision-making tree; $h_n(x)$ is the prediction pattern of the $n_{th}$ decision-making tree; and $A_{i,j}^{d}(x)$ is the odds of $j$ land use pattern growth at the spatial module $i$. Here, $A_{i,j}$ indicates the expansion odds of LUCC type $j$ at position $i$; the merit of $d$ is 1 or 0, where 1 indicates that other types of conversion to type $j$ have taken place, and 0 indicates no transition; $x$ is the complexor of the drive; $I(h_n(x) = d)$ is the pointer ability of the set of decision-making trees; $h_n(x)$ is the prediction type of the $n_{th}$ decision-making tree of complexor $x$; and $M$ is the overall figure of decision-making trees.

The cellular automata (CA) model involves LUCC competition by employing an attuned element to attain the necessary number of any pattern of patch. Meanwhile, the cohesion of multi-type stochastic plaque seeds and a decreasing threshold enables the spatiotemporal dynamic simulation for the automatic generation of LUCC plaques. The equation for the CA model is as below [42]:

$$OP_{i,j}^{d=1,t} = P_{i,j}^{d} \times \Omega_{i,j}^{t} \times D_{j}^{t} \quad (4)$$

In the formula, $OP_{i,j}^{d=1,t}$ is the comprehensive likelihood of the alteration of the spatial module $i$ to the land class $j$ at the $t$ moment, $P_{i,j}^{d}$ is the apposite likelihood of the development of the land type $i$ at the spatial module $j$, $D_{j}^{t}$ is the influence of the future requirement on the land class $j$, and $\Omega_{i,j}^{t}$ is the vicinity spillover of the module $i$. It is the coverage proportion of the land use constituents of the land class $j$ in the other vicinity [43].

In this paper, the parameters for the random forest regression are set as follows: the default number of random forests is 20; the default sampling rate is 0.01, which means that 1% of the pixels will be used for model training. Neighborhood weight refers to the influence range of each land type on the neighborhood, ranging from 0 to 1. By calculating the number of pixels of each land type in 2020 and the total number of changed pixels of each land type in 2030 predicted by the Markov chain, the ratio of the number of changed pixels of each land type to the total number of changed pixels in the simulated area is calculated as the neighborhood weight. Based on the four different development scenarios, the following parameter list of neighborhood weights with high simulation accuracy is finally set, see Table 3.

**Table 3.** Neighborhood weights of simulation scenarios.

| | Cropland | Forest | Grassland | Water | Built-Up Land | Unused Land |
|---|---|---|---|---|---|---|
| BAU | 0.4285 | 0.3134 | 0.1378 | 0.0181 | 0.1081 | 0.0001 |
| UD | 0.4246 | 0.3126 | 0.1369 | 0.0180 | 0.1076 | 0.0003 |
| CP | 0.4401 | 0.3143 | 0.1384 | 0.0183 | 0.0886 | 0.0003 |
| EP | 0.4270 | 0.3273 | 0.1340 | 0.0181 | 0.0935 | 0.0001 |

To enhance the precision of predicting later land use patterns in Liaoning Province, we made use of land use status information between 2000 and 2010 to predict the land use situation in 2020 using the PLUS model. Subsequently, we validated the results against actual data. The Kappa coefficient can test the overall consistency between the simulation results of the PLUS model and actual data. The formula for the Kappa coefficient is as follows:

$$Kappa = \frac{P_o - P_c}{P_p - P_c} \quad (5)$$

Here, $P_o$ is the ratio of correctly simulated grid cells; in this paper, land use types are divided into 6 categories, so $P_c = 1/6$; $P_p$ is the percentage of correctly simulated grid cells in the ideal state, which is 100%. The Kappa coefficient ranges from $-1$ to 1, and it is generally considered that Kappa > 0.6 indicates significant consistency, while Kappa > 0.8 means the simulation effect is better.

The analysis revealed a Kappa coefficient of 0.76, indicating a collective precision of 83.88%. The FoM value is 0.023, which is within the range of 0.01–0.25, and at the same time, a Kappa coefficient closer to 1 signifies better consistency of the model, suggesting that the predicted land use data closely align with the true data. These results underscore the high confidence and precision of the PLUS model, affirming its suitability for simulating land use types in Liaoning Province.

## 3. Setting of Development Scenarios

Based on the land use change observed in the study range, the below-mentioned four scenarios have been established to predict the land use pattern of Liaoning Province in 2030:

- Business-as-usual scenario: under this scenario, the elements influencing land use variety in Liaoning Province remain relatively stable, and land use change continues along the development trend observed from 2000 to 2020.
- Urban development scenario: in this scenario, land allocation prioritizes urban construction, resulting in an increased likelihood of transition of arable land, woodland, and grassland to impervious land [44]. Specifically, the convert odds of grassland, arable land, and woodland to impervious land are augmented by 20%, while the convert odds of impervious land to other land patterns, except cropland, are lowered by 60%.

- Cropland protection scenario: under this scenario, Liaoning Province implements the national conservation tillage plan to safeguard cropland, which is crucial for food security [45]. The objective is to curtail the transition of arable land to other land types. The convert likelihood of arable land to impervious land is diminished by 60%.
- Ecological protection scenario: in this scenario, LUCC is managed through measures such as reverting arable land to woodland and grassland, closing mountains, and banning grazing. The convert odds of specific land patterns are adjusted as follows [46]: the convert odds of woodland and grassland to impervious land are dwindled by 50%, the convert odds of arable land to impervious land are declined by 30%, and the convert odds of arable land and grassland to woodland are raised by 30%.

#### 2.3.4. Carbon Reserve Estimated by InVEST Model

The InVEST model includes the carbon module, which is capable of deducing the computation and transversion of a carbon reserve, presuming that it is quiescent and does not alter over time. The carbon reserve in ecosystems is separated into the four essential carbon pools. Table 2 denotes the carbon densities for various LUCC types, including aboveground biological carbon density, underground biological carbon density, soil organic matter carbon density, and dead organic matter carbon density. The equations used for estimation are as follows [47]:

$$C_{total} = C_{above} + C_{below} + C_{soil} + C_{dead} \quad (6)$$

$$C_t = \sum_{i=1}^{n} A_k \times C_k (k = 1, 2, \cdots, n) \quad (7)$$

$C_{total}$ is the overall carbon reserve of the study range; $C_{above}$ is the aboveground biological carbon reserve; $C_{below}$ is the underground biological carbon reserve; $C_{soil}$ is the soil organic matter carbon reserve; and $C_{dead}$ is the dead organic matter carbon reserve. Here, $C_k$ is the amount of carbon stored for each LUCC type; $C_t$ is the quantity of carbon reserved in assigned module; and $A_k$ is the range of a particular LUCC type.

## 3. Results

### *3.1. Land Use Changes in Liaoning Province*

#### 3.1.1. Dynamic Changes in Land Use from 2000 to 2020

From 2000 to 2020, cropland remained the preponderant land use type in Liaoning Province, covering 47.84% of the overall zone, primarily concentrated in the central plains. Forests accounted for 28.93% of the collective proportion. Grasslands occupied 14.14% of the overall square measure. Impervious land was primarily scattered in the Liaohe Plain, spanning between the hills of eastern and western Liaoning (Table 4). From a spatial viewpoint, distinct land use/cover change characteristics were observed in Liaoning Province due to varied topographical conditions. Forest expansion was chiefly noted in the eastern and central zones, while grassland growth occurred predominantly in the low mountainous and hilly areas of northwestern Liaoning. The increase in water domains was preponderantly observed in the Daling River and northern Bohai Sea. Conversely, the construction land of the Liaohe Plain expanded by a wide margin, situated between the hills of eastern and western Liaoning in Figure 3.

**Table 4.** Land use change in Liaoning Province from 2000 to 2020.

| Year | Cropland | | Forest | | Grassland | | Water | | Built-Up Land | | Bare Land | |
|---|---|---|---|---|---|---|---|---|---|---|---|---|
| | km$^2$ | % | km$^2$ | % | km$^2$ | % | km$^2$ | % | km$^2$ | % | km$^2$ | % |
| 2000 | 72,566.19 | 49.41 | 41,841.09 | 28.49 | 20,764.44 | 14.14 | 2952.72 | 2.01 | 8713.71 | 5.93 | 0.09 | 0.02 |
| 2010 | 71,367.57 | 48.71 | 41,702.22 | 28.46 | 20,852.46 | 14.23 | 3043.35 | 2.07 | 9536.49 | 6.50 | 1.08 | 0.03 |
| 2020 | 67,004.91 | 45.4 | 44,040.69 | 29.84 | 20,732.13 | 14.04 | 3167.01 | 2.14 | 12627 | 8.55 | 2.61 | 0.03 |

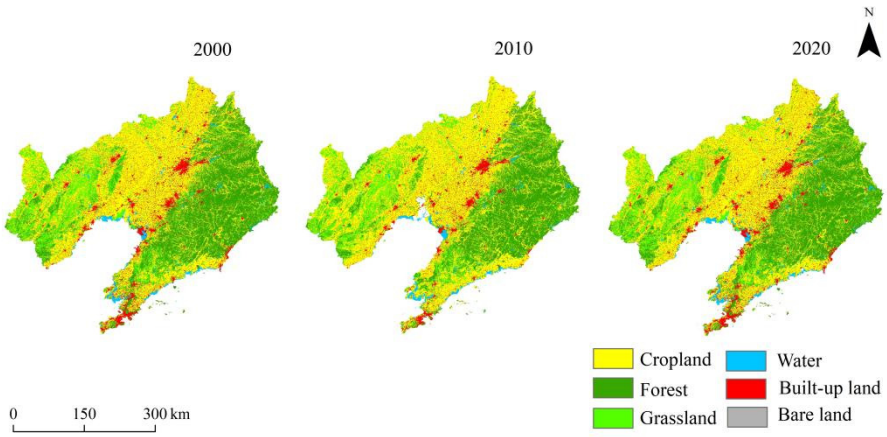


**Figure 3.** Distribution of LUCC in the Liaoning Province from 2000 to 2020.

A chord diagram was employed to quantitatively describe the orientation and diversity of the transformation of different LUCC patterns in different periods. As depicted in Figure 4, over the past two decades, Liaoning Province has undergone noticeable transformations in land use patterns, with a collective square measure of 146,508.50 km$^2$ transitioning (Table 5). During this period, from the viewpoint of "turning", the most notable characteristic of land use alteration in the province was the increase in forested areas. Over the past 20 years, a collective of 6208.01 km$^2$ of various land patterns were converted into forest, of which 3671.03 km$^2$ originated from cropland, constituting 59% of the total conversion. Following forest, grassland witnessed the next utmost increment in range, with an overall conversion area of 4621.76 km$^2$, predominantly sourced from forest, with forest-to-grassland conversions totaling 2330.04 km$^2$, accounting for 50.41%. The new area of impervious land is 4492.28 km$^2$, which is preponderantly from cropland, accounting for 3732.31 km$^2$, accounting for 83.08%.

**Table 5.** Land use transfer matrix of Liaoning Province from 2000 to 2020.

| **Year** | | | | **2020** | | | |
|---|---|---|---|---|---|---|---|
| **2000** | **Cropland** | **Forest** | **Grassland** | **Water** | **Built-Up Land** | **Bare Land** | **Total** |
| Cropland | 62,577.16 | 3671.03 | 2150.30 | 322.11 | 3732.31 | 45.11 | 72,498.02 |
| Forest | 1478.04 | 37,737.64 | 2330.04 | 39.39 | 154.43 | 1.54 | 41,741.07 |
| Grassland | 1881.23 | 2442.02 | 15,950.19 | 62.63 | 326.75 | 16.87 | 20,679.70 |
| Water | 276.48 | 55.43 | 87.15 | 2156.74 | 278.79 | 5.52 | 2860.11 |
| Built-up land | 675.00 | 39.53 | 54.19 | 14.70 | 7945.60 | 0.45 | 8729.47 |
| Bare land | 0.01 | 0.00 | 0.08 | 0.00 | 0.00 | 0.04 | 0.13 |
| Total | 66,887.92 | 43,945.66 | 20,571.95 | 2595.57 | 12,437.88 | 69.52 | 146,508.50 |

From the perspective of "turning out", the most remarkable characteristic of land use alteration in the province was the reduction in cropland area. Over the 20 years in question, an overall of 9920.86 km$^2$ of cropland was converted into other land patterns, primarily into impervious land and forest, covering areas of 3732.31 km$^2$ and 3671.03 km$^2$, respectively. Grassland conversion ranked second, with an overall conversion proportion of 4729.50 km$^2$, of which grassland-to-forest conversions accounted for 2442.02 km$^2$, or 51.63%. The results indicate that the developmental trend of land use patterns in Liaoning Province between 2000 and 2020 witnessed the expansion of impervious land at the sacrifice of arable land and grassland.

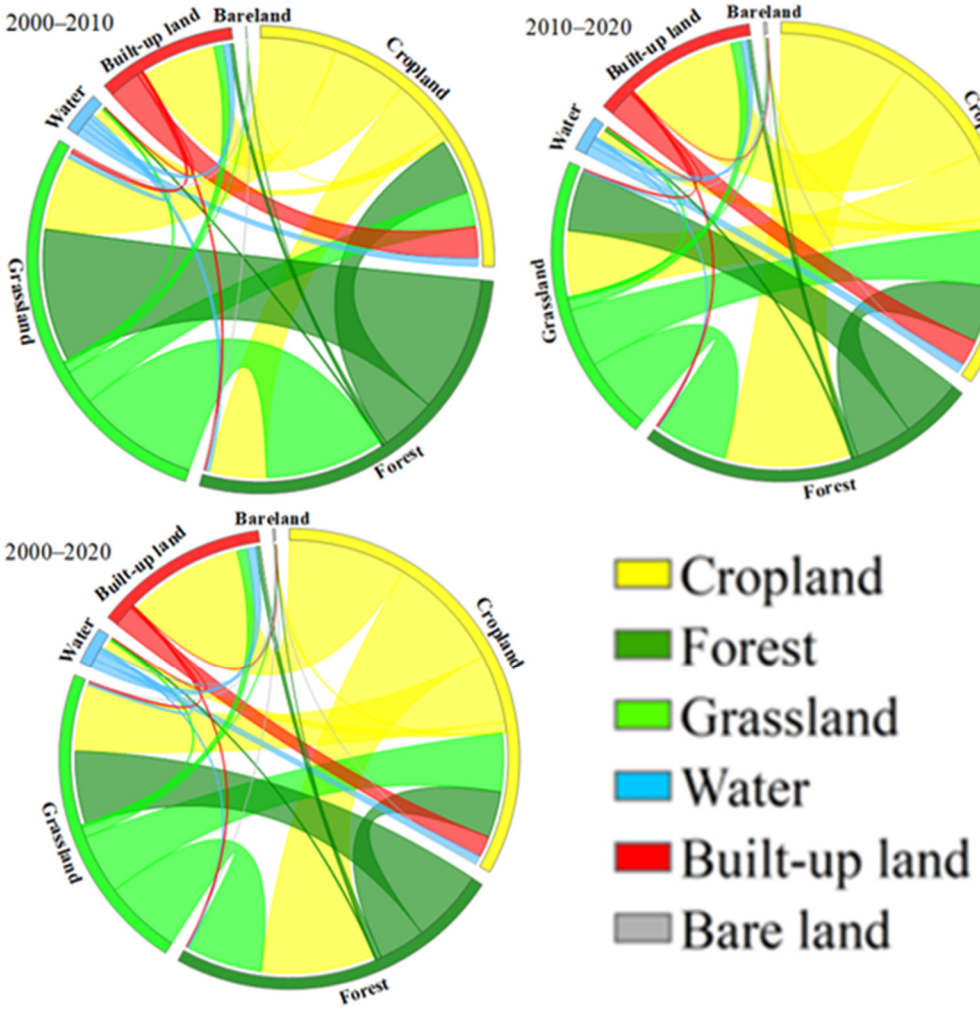


**Figure 4.** Transfer matrix of LUCC changes in Liaoning Province from 2000 to 2020.

3.1.2. Dynamic Changes in Land Use from 2020 to 2030

Based on the LUCC data of Liaoning Province in 2020, the validated PLUS model was utilized to calculate the LUCC distribution map of 2030 under different scenarios in Figure 5. In the light of the prediction outcome, under the scenario of business as usual, compared with 2020 (Table 6), there was a prominent rise in the proportion of woodland and impervious land in Liaoning Province, expanding by 1796.05 km$^2$ and 2380.38 km$^2$, respectively. Notably, the increase speed of impervious land was the most pronounced, exhibiting the highest growth rate and accounting for an increase of 17.88%. Regarding land use transitions, the new impervious land predominantly originated from cultivated land and meadow land, while the new forest mainly resulted from grassland conversion. Spatially, the growth in forest was concentrated in Jinzhou City in the focal and western segment of Liaoning Province. Land use type conversions were predominantly distributed near the Liaohe River Plain, exhibiting patterns similar to those observed in the last two decades.

Under the urban development scenario, compared with 2020, there was a remarkable enhancement in the zone of impervious land and forest in Liaoning Province, expanding by 3106.7 km$^2$ and 1662.02 km$^2$, respectively. Notably, the increment in construction land was the most pronounced, with a cumulative increase of 24.6%. In terms of land conversion, a substantial amount of arable land, woodland and grassland was switched over to impervious land. Spatially, the increment in impervious land was preponderantly concentrated in Shenyang in the middle of Liaoning Province and Dalian in the south. Compared with the business-as-usual scenario, the trends of increase and decrease in

land types remained consistent, with a remarkable enhancement in the proportion of construction land, rising by 6.72%.

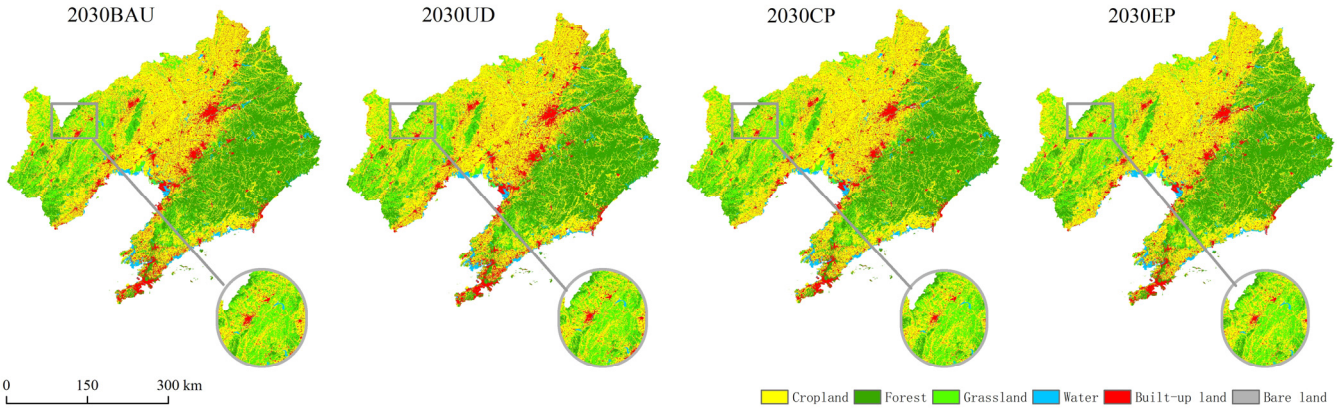


**Figure 5.** Land use and cover change (LUCC) by 2030.

**Table 6.** Land area by 2030 by assuming the following scenarios: BAU, UD, CP, and EP ($km^2$).

| | 2020 | 2030BAU | 2030UD | 2030CP | 2030EP |
|---|---|---|---|---|---|
| Cropland | 67,004.91 | 62,647.56 | 62,071.12 | 64,389.95 | 62,403.12 |
| Forest | 44,040.69 | 45,823.05 | 45,702.71 | 45,940.51 | 47,842.44 |
| Grassland | 20,732.13 | 20,156.76 | 20,024.37 | 20,225.32 | 19,596.55 |
| Water | 3167.01 | 2660.22 | 2640.32 | 2669.51 | 2657.17 |
| Built-up land | 12,627 | 14,884.38 | 15,733.70 | 12,946.67 | 13,672.74 |
| Bare land | 2.61 | 2.61 | 2.35 | 2.61 | 2.56 |
| Area | 147,574.35 | 146,174.58 | 146,174.58 | 146,174.58 | 146,174.58 |

Under the cropland protection scenario, compared with 2020, there was a remarkable increment in both cropland and woodland in Liaoning Province, with additions of 2385.04 $km^2$ and 1899.82 $km^2$, respectively. Notably, the area of cropland saw the most substantial increase, with a cumulative growth of 3.6%, while the decrease in impervious land was the largest, with a cumulative decrease of 37.1%. From a conversion perspective, the trend primarily reflects mutual transformations between impervious land and cropland. Spatially, the increased cropland area is predominantly focused on the focal Liaohe Plain. Compared with the business-as-usual and urban development scenarios, the change trend of woodland, grassland, and water remained consistent, with cropland area increasing by 9.23% and 10.96%, and built-up land area significantly decreasing by 54.98% and 61.7%, respectively.

Under the ecological protection scenario, compared with 2020, there will be a noteworthy augment in woodland and meadow land in Liaoning Province, with additions of 4801.75 $km^2$ and 164.42 $km^2$, respectively. The forest area sees the largest increase, with a cumulative growth of 10.9%, while the impervious land range experiences the most significant decrease, with a cumulative decline of 17.85%. In terms of land conversion, the notable trend is the substantial increase in forest area. Spatially, the expanded forest zone is primarily concentrated in the low mountain and hilly domains in the west of Liaoning Province. Compared with the scenario of business as usual, the ratio of forest increases by 6.82%. Compared with the urban development scenario, the scale of impervious land decreases by 42.45%. Compared with the cropland protection scenario, the ratio of grassland increases by 3.23% and the proportion of cropland decreases by 8.98%.

### *3.2. Dynamic Changes in Carbon Reserves in Liaoning Province*

#### 3.2.1. Dynamic Changes in Carbon Reserves from 2000 to 2020

The carbon reserve of Liaoning Province in 2000, 2010, and 2020 was 1417.59 Tg C, 1412.87 Tg C, and 1448.11 Tg C, respectively (Table 7). Among them, the carbon reserve decreased by 4.72 Tg C from 2000 to 2010, with a reduction ratio of 0.33%. From 2000 to 2020, the spatial spread pattern of the carbon reserve in Liaoning Province demonstrates a spatial spread type of "high–low–high" from east to west, indicating the spatial aggregation features of "high in the east and low in the west".

Among them, in Figure 6, the high carbon reserve is mainly distributed in eastern Liaoning, such as in Tieling City, Fushun City, and Dandong City, with a carbon reserve of more than 241.35 tons per unit area. The preponderant land use patterns in these zones are woodland and grassland, with a strong carbon sequestration capacity. A low carbon reserve is primarily scattered in the central plain regions such as Shenyang, Jinzhou, Liaoyang, and Panjin.

From a spatial perspective, based on the alteration of the carbon reserve in a piece of a grid cell, the spatial pattern of carbon reserves is obtained in Figure 7, which is divided into "carbon source", "carbon balance", and "carbon sink". In the 20 years in question, the increasing regions of carbon reserve are predominantly focused in the eastern woodland and western grassland, while the decreasing areas of carbon reserve are principally distributed in Shenyang and Panjin in the middle.

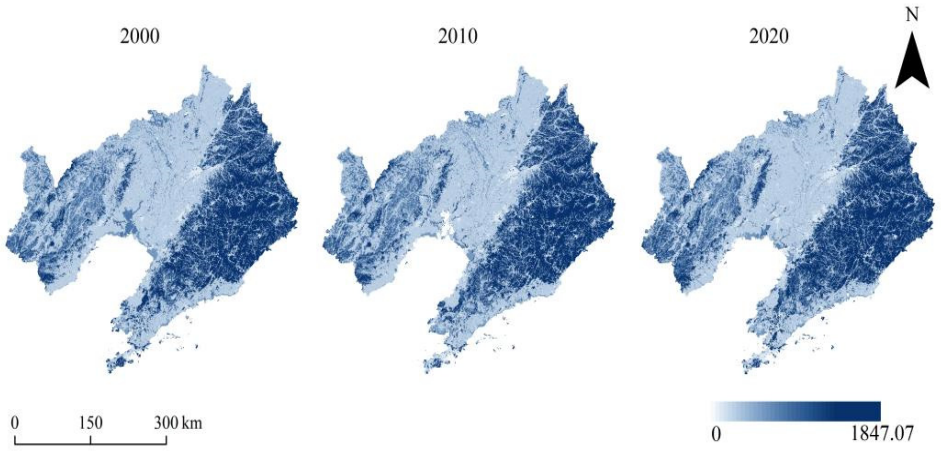


**Figure 6.** Distribution of carbon reserve in Liaoning Province from 2000 to 2020.

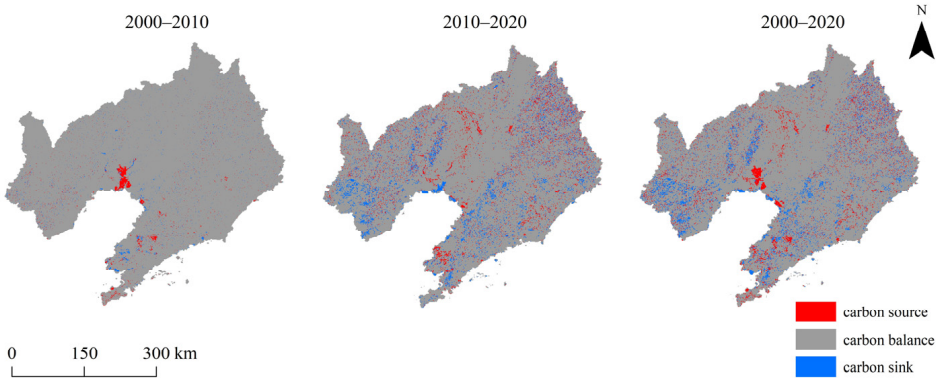


**Figure 7.** Distribution of carbon reserve changes in Liaoning Province during different periods.

**Table 7.** Carbon reserves in Liaoning province from 2000 to 2020 (Tg C).

| Year | Cropland | Forest | Grassland | Water | Built-Up Land | Bare Land | Total |
|---|---|---|---|---|---|---|---|
| 2000 | 277.56 | 856.98 | 246.72 | 24.56 | 11.76 | 0.00 | 1417.59 |
| 2010 | 272.99 | 853.76 | 247.93 | 25.33 | 12.87 | 0.00 | 1412.87 |
| 2020 | 256.44 | 902.24 | 246.08 | 26.34 | 17.00 | 0.00 | 1448.11 |

3.2.2. Dynamic Changes in Carbon Reserves in 2020–2030

Under the scenario of business as usual, the carbon reserve of Liaoning Province in 2030 is 1449.35 Tg C, which is 1.24 Tg C more than that in 2020 in Table 8. Compared with 2020, low-value regions of carbon reserve are primarily focused in the focal part of Liaoning Province, characterized by cultivated land and construction land, while high-value zones of carbon reserve are principally found in the mountainous districts of eastern Liaoning and the low hilly regions of western Liaoning, dominated by forest and grassland in Figure 8. Spatially, in Figure 9, during the 10-year period, the augment in carbon reserve was chiefly focused in Jinzhou City in the focal and western part of Liaoning Province, primarily due to significant forest area expansion resulting from the transformation of numerous grasslands into woodland, thereby increasing carbon reserve content (Table 9).

Under the scenario of urban development, the carbon reserve of Liaoning Province in 2030 is 1413.54 Tg C, which is 34.56 Tg C less than that in 2020, with a decrease of 2.39% in Table 8. Compared with 2020, an expanded range of low-value carbon reserve zones is primarily scattered in the focal flatlands and southern littoral regions of Liaoning Province, dictated by built-up land. The distribution of high-value carbon reserve ranges remains largely unchanged in Figure 8. Spatially, in Figure 9, during the 10-year period, the reduced carbon reserve was centralized in the focal plains of Liaoning Province, attributed to vigorous economic development and accelerated dilation of various construction land types. Compared with the business-as-usual scenario, the carbon reserve under this scenario is reduced by 35.81 Tg C (Table 9).

Under the scenario of cropland protection, the carbon reserve of Liaoning Province in 2030 is 1450.39 Tg C, which is 2.28 Tg C more than that in 2020. The spatial spread of the carbon reserve remains basically unchanged compared with 2020 in Table 8. Low-merit regions of carbon reserves are chiefly distributed in the focal Liaohe Plain, while high-value zones of carbon reserve are basically found in the mountainous domains of eastern Liaoning and the low mountain and hilly scopes of western Liaoning in Figure 8. Spatially, in Figure 9, during the 10-year period, the increased carbon reserve was focused in Shenyang in the central part of Liaoning Province. Compared with the business-as-usual scenario, the carbon reserve in this scenario is reduced by 1.04 Tg C, indicating a weaker carbon sequestration capacity of cropland compared to forest and grassland. Compared with the urban development scenario, the carbon reserve in this scenario increased by 36.85 Tg C Table 9.

**Table 8.** Carbon reserves of Liaoning Province in 2030 (Tg C).

| | 2020 | 2030BAU | 2030UD | 2030CP | 2030EP |
|---|---|---|---|---|---|
| Cropland | 256.44 | 247.79 | 252.53 | 256.77 | 253.13 |
| Forest | 902.24 | 915.30 | 875.19 | 906.16 | 938.88 |
| Grassland | 246.08 | 239.87 | 238.29 | 244.11 | 236.44 |
| Water | 26.34 | 26.37 | 26.37 | 26.37 | 26.37 |
| Built-up land | 17.00 | 20.02 | 21.16 | 16.98 | 16.98 |
| Bare land | 0.00 | 0.00 | 0.00 | 0.00 | 0.00 |
| Total | 1448.11 | 1449.35 | 1413.54 | 1450.39 | 1471.81 |

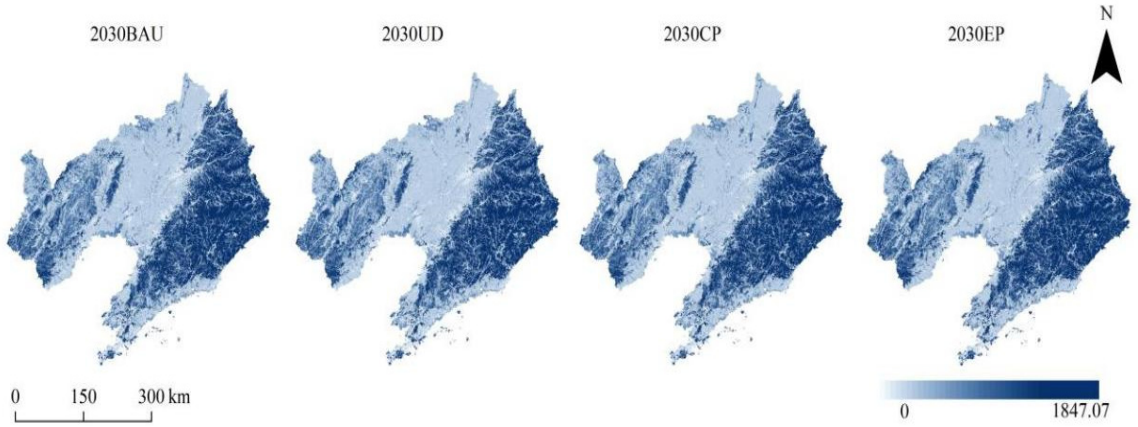


**Figure 8.** Spatial distributions of carbon reserves in Liaoning Province in 2030.

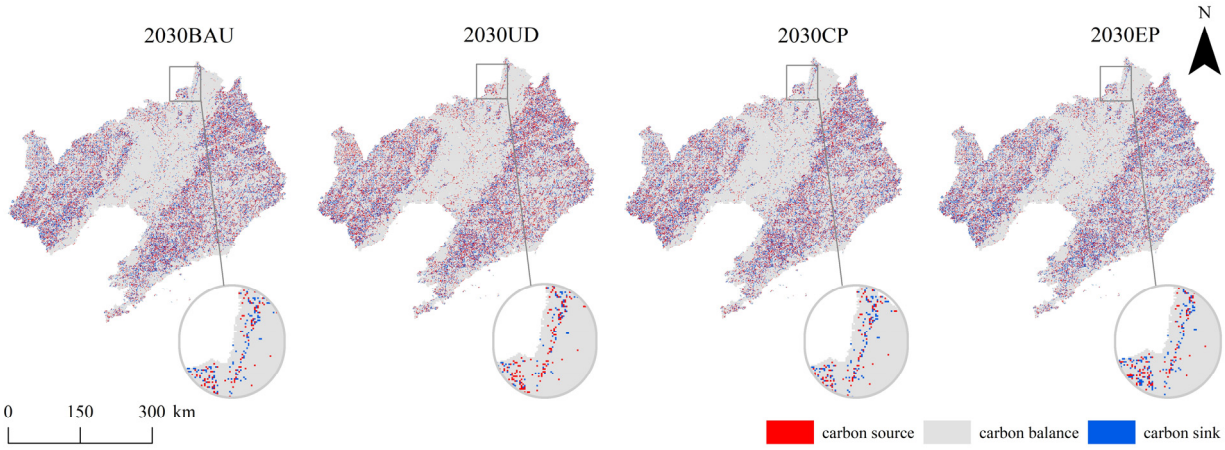


**Figure 9.** Spatial changes in carbon storage in Liaoning Province from 2020 to 2030.

**Table 9.** Change in carbon reserve from 2020 to 2030 (t).

| | 2030BAU | 2030UD | 2030CP | 2030EP |
|---|---|---|---|---|
| Cropland | −8.65 | −3.91 | 0.33 | −3.30 |
| Forest | 13.06 | −27.05 | 3.92 | 36.64 |
| Grassland | −6.22 | −7.79 | −1.98 | −9.65 |
| Water | 0.03 | 0.03 | 0.03 | 0.03 |
| Built-up land | 3.02 | 4.16 | −0.02 | −0.02 |
| Bare land | 0.00 | 0.00 | 0.00 | 0.00 |
| Total | 1.24 | −34.57 | 2.28 | 23.70 |

Under the scenario of ecological protection, the carbon reserve of Liaoning Province in 2030 is 1471.80 Tg C, an increase of 23.69 Tg C compared to that in 2020, representing a 1.64% increase in Table 8. Compared with 2020, the spatial distribution of the carbon reserve has converted prominently, with an expanded range of high-value carbon reserve domains primarily scattered in the mountainous areas of eastern Liaoning and the low hilly regions of western Liaoning in Figure 8. Spatially, in Figure 9, during the 10-year period, the increased carbon reserve was focused in the low mountain and hilly areas of western Liaoning Province, western parts of Chaoyang City, Huludao City and so on. Compared with the business-as-usual scenario, the carbon reserve in this scenario increased by 22.45 Tg C in Table 9. Compared with the urban development scenario, the carbon

reserve in this scenario increased by 58.26 Tg C, mainly concentrated in the focal plains and southern coastal domains. Compared with the cropland protection scenario, the carbon reserve in this scenario increased by 21.41 Tg C.

## 4. Discussion

### *4.1. Impact of LUCC on Carbon Reserves in Liaoning Province*

The impact and driving mechanisms of land use/cover change on carbon reserves in terrestrial ecological systems have become a focal point in contemporary society [48]. The variations in land use cover in Liaoning Province between 2000 and 2020 significantly affected the regional carbon reserve. During this period, the carbon reserve capacity exhibited notable spatial heterogeneity, with higher merits in mountainous zones and minor hilly regions dominated by forest and grassland ecosystems, and lower values in central agricultural areas and densely urbanized coastal zones.

Currently, a great many savants [4] argue that the transformation of the built-up land of cultivated land to woodland in China has effectively increased the overall carbon reserve capability [49]. Consequently, the increment in carbon reserves in Liaoning Province mainly stems from afforestation (net increase of 30.52 Tg C), making it a promising region for carbon reserves and resource enrichment [50]. If forest areas are concentrated in areas with low-lying populace consistency and minimal human activity, a substantial expansion of woodland results in a corresponding increase in carbon reserves. Xie et al. [51] examined the space–time continuum evolution of land use variation and carbon reserves in Chengdu between 1990 and 2020, concluding that improvements in forest area and quality have enhanced carbon reserves. Chen et al. [52] analyzed LUCC effects on carbon pools in Central Asia from 1975 to 2005, highlighting carbon sequestration as a significant outcome, particularly in forested areas. Thus, woodland has a significant role in augmenting regional carbon reserve capability.

In Liaoning Province, most built-up land is situated in central plains and southern coastal areas. Urbanization inevitably sacrifices built-up land to accommodate urban expansion. However, urban dilation at the expense of cultivated land is a principal element contributing to the province's declining zonal carbon reserve capability. While urban dilation may seem beneficial initially, it could substantially diminish the province's ecosystem carbon reserve capability in the long term [53]. Zhang et al. [54] observed a descending tendency in ecosystem carbon reserves in Taiyuan City over 30 years from 2000 to 2030 due to reduced cropland and rapid expansion of artificial land surfaces, highlighting the spillover of land use/cover type variations on zonal ecological system carbon reserves.

### *4.2. Impacts of Distinct Advancement Circumstances on Carbon Reserves in Liaoning Province*

Under the scenario of business as usual, Liaoning Province will continue its current trajectory of land use progression, leading to a total carbon reserve increase of 1.24 Tg C by 2030. Despite a prominent dilation of impervious land, ongoing efforts by the Liaoning provincial government to promote ecological construction and protection, as outlined in the Circular of the State Council by issuing the 13th five-year Plan for Ecological Environmental Protection, are expected to enhance forest cover and implement greening initiatives in urban built-up areas, consequently boosting the province's total carbon reserves. Under the scenario of urban development, the dilation of impervious land encroaches upon arable land, woodland, grassland, and other ecological land, giving rise to a descending tendency in Liaoning Province's carbon reserves [55]. By 2030, carbon reserves are projected to decrease by 34.56 Tg C compared to 2020. Under the cropland protection scenario, emphasis is placed on preserving cropland areas and effectively restraining cropland reduction. This scenario aims to mitigate the loss of cropland and its associated carbon reserves.

The ecological protection scenario counters the declining tendency that forest area observed in business-as-usual scenarios, thereby improving carbon reserve services in Liaoning Province. This scenario results in a significant rise in Liaoning Province's carbon reserves, showcasing a "high–low–high" space pattern and "high in the east and low-

level in the west" spatial aggregation characteristics [13]. Further research is warranted to optimize ecological and economic benefits. These findings align with prior research; for instance, Zhu et al. [56] examined space–time continuum variations in carbon reserves in the littoral of Liaoning Province from 1995 to 2018, noting higher carbon reserves scattered on the east and west sides, consistent with this study. Similarly, Lu [57] analyzed the space pattern characteristics of ecological system land conservation functions in Liaoning Province, observing higher soil organic carbon reserves in the eastern mountainous zone, followed by the mountainous and hilly region of western Liaoning, and lower levels in the central plain.

### *4.3. Limitations*

This study primarily delves into understanding the relation between land use/cover change and carbon reserves. While the simulation outcomes offer theoretical insights for areal advancement and land use strategy, certain limitations warrant acknowledgment. Firstly, the InVEST model simplifies to a large extent the carbon loop process by postulating linear variations in carbon reserves over time and fixed carbon density data [46]. However, carbon density values may exhibit spatial heterogeneity, potentially overlooking carbon fluctuations resulting from seasonal variations and vegetation age [58]. The utilization of carbon density data from previous studies introduces uncertainty into the robustness of the results, given discrepancies in scholars' interpretations and regional carbon density knowledge [26]. Addressing this limitation in prospective explorations is imperative to enhance carbon reserve estimation accuracy.

Looking ahead to land use simulations of future tendencies, the study presents four scenarios, yet acknowledges inherent uncertainties. Firstly, the PLUS model's fixed conversion rules may not accurately capture future land use changes, as areal progression programming and policy demands could not immediately switch due to model-constrained regulation. Given the prominent bearing of local policies on land use patterns, optimizing LUCC simulation outcomes becomes imperative. Furthermore, while this study identifies ten driving factors for future land use changes, the actual drivers are often more complex and diverse. Therefore, future research should delve deeper into potential driving factors, incorporate local government's medium-to-long-term development planning into constraint rules, and integrate innovative methodologies with the PLUS model. Adjusting model arguments and transformation rules can augment the exactitude of later land use change simulations [59].

## 5. Conclusions

Using the PLUS and InVEST models as research methods, we analyzed the coordination relationship between the change in the patterns of land use and the carbon reserves of Liaoning Province between 2000 and 2020. Building upon this analysis, the variations in carbon reserves in four circumstances in 2030 were simulated through variations in LUCC types, and recommendations were proposed for zonal progression. The principal conclusions are as below:

(1) During the period from 2000 to 2020, land use patterns in Liaoning Province were primarily characterized by the mutation of cultivated land to impervious land. During this period, affected by the interplay of different LUCC types, carbon reserves initially declined before rebounding, resulting in a cumulative increase of 30.52 Tg C.

(2) Land use simulation results indicate that forest area preservation is prioritized in the ecological protection circumstance, with a 3801.45 $km^2$ increase compared to 2020, while built-up land growth slows. The carbon reserve value of the whole province in the ecological conservation circumstances for 2030 will increase by 23.69 Tg C.

Within the "double carbon" target, ecological protection emerges as the optimal path for Liaoning Province's future planning. Liaoning Province should give full play to the advantages of its own regions according to different resources and socioeconomic conditions. In future development and construction, ecological resources should be strictly

protected. Hence, forests, as vital ecological resources, require enhanced protection to bolster their greenhouse gas purification capacity. At the same time, the development intensity of the Liaohe Plain and coastal land should be reasonably controlled to improve the intensive economic ability of construction land. This study is of reference value for optimizing inter-provincial land use spatial distribution and formulating low-carbon development strategies.

**Author Contributions:** Conceptualization, H.G.; software, J.L.; validation, H.G. and J.L.; supervision, S.W. and H.G.; resources, H.G.; data curation, H.G. and J.L.; writing—original draft, J.L.; writing—review and editing, S.W., H.G. and J.L.; project administration, S.W. and H.G.; funding acquisition, H.G. All authors have read and agreed to the published version of the manuscript.

**Funding:** This research was funded by the Ministry of Education Humanities and Social Sciences General Research Project (grant number: 23A10157004), Liaoning Provincial Department of Education, Social Science Project, Study on the Decoupling Relationship between Land Use Efficiency and Carbon Emission and its Realization Path in Three Eastern Provinces in the Context of New Urbanization (grant number: JYTQN2024019), Liaoning Provincial Department of Science and Technology, Qingyuan County Ground Power Enhancement Science and Technology Mission, Liaoning Province(grant number: 2024JH5/10400158), Propaganda Department of Liaoning Provincial Committee of the Communist Party of China, "Xingliao Talent Program" "Cultural Masters" and "Four Batch" Talents (grant number: XLYC2210046).

**Institutional Review Board Statement:** Not applicable.

**Informed Consent Statement:** Not applicable.

**Data Availability Statement:** Data is contained within the article.

**Acknowledgments:** We thank the editors and anonymous reviewers who provided comments and suggestions for further improvement; in addition, Jiabin Li would like to thank Gu Hanlong and Wang Shuai for their strong support for this article.

**Conflicts of Interest:** The authors declare no conflicts of interest.

## References

1. Yin, Z.; Feng, Q.; Zhu, R.; Wang, L.; Chen, Z.; Fang, C.; Lu, R. Analysis and Prediction of the Impact of Land Use/Cover Change on Ecosystem Services Value in Gansu Province, China. *Ecol. Indic.* **2023**, *154*, 110868. [CrossRef]
2. Dong, J.; Guo, Z.; Zhao, Y.; Hu, M.; Li, J. Coupling Coordination Analysis of Industrial Mining Land, Landscape Pattern and Carbon Storage in a Mining City: A Case Study of Ordos, China. *J. Geo. Nat. Haz. Risk* **2023**, *14*, 2275539. [CrossRef]
3. Li, Z.; Xia, J.; Deng, X.; Yan, H. Corrigendum to 'Multilevel Modelling of Impacts of Human and Natural Factors on Ecosystem Services Change in an Oasis. *Resour. Conserv. Recycl.* **2021**, *174*, 105791. [CrossRef]
4. Chang, X.; Xing, Y.; Wang, J.; Yang, H.; Gong, W. Effects of Land Use and Cover Change (LUCC) on Terrestrial Carbon Stocks in China between 2000 and 2018. *Resour. Conserv. Recycl.* **2022**, *182*, 106333. [CrossRef]
5. Liu, X.; Ye, Y.; Ge, D.; Wang, Z.; Liu, B. Study on the Evolution and Trends of Agricultural Carbon Emission Intensity and Agricultural Economic Development Levels—Evidence from Jiangxi Province. *Sustainability* **2022**, *14*, 14265. [CrossRef]
6. IPCC. Climate Change and Land: An IPCC Special Report on Climate Change, Desertification, Land Degradation, Sustainable Land Management, Food Security, and Greenhouse Gas Fluxes in Terrestrial Ecosystems. Available online: https://www.ipcc.ch/report/ar6/wg2/resources/press/press-release-chinese/ (accessed on 23 March 2022).
7. Stankovic, M.; Ambo-Rappe, R.; Carly, F.; Dangan-Galon, F.; Fortes, M.D.; Hossain, M.S.; Kiswara, W.; Van Luong, C.; Minh-Thu, P.; Mishra, A.K.; et al. Quantification of Blue Carbon in Seagrass Ecosystems of Southeast Asia and Their Potential for Climate Change Mitigation. *Sci. Total Environ.* **2021**, *783*, 146858. [CrossRef]
8. Zhao, Y.; Dong, Y.; Liu, P. Predicting Low Carbon Pathways on the Township Level in China: A Case Study of an Island. *Environ. Monit. Assess.* **2024**, *196*, 150. [CrossRef]
9. Wang, L.; Zhu, R.; Yin, Z.; Chen, Z.; Fang, C.; Lu, R.; Zhou, J.; Feng, Y. Impacts of Land-Use Change on the Spatio-Temporal Patterns of Terrestrial Ecosystem Carbon Storage in the Gansu Province, Northwest China. *Remote Sens.* **2022**, *14*, 3164. [CrossRef]
10. Gao, L.; Tao, F.; Liu, R.; Wang, Z.; Leng, H.; Zhou, T. Multi-Scenario Simulation and Ecological Risk Analysis of Land Use Based on the PLUS Model: A Case Study of Nanjing. *J. Sustain. Cities Soc.* **2022**, *85*, 104055. [CrossRef]
11. NDRCC. *Enhanced Actions on Climate Change: China's Intended Nationally Determined Contributions*; Department of Climate Change, National Development and Reform Commission of China: Beijing, China, 2015.
12. Chanapathi, T.; Thatikonda, S. Investigating the Impact of Climate and Land-Use Land Cover Changes on Hydrological Predictions over the Krishna River Basin under Present and Future Scenarios. *Sci. Total Environ.* **2020**, *721*, 137736. [CrossRef]

13. Sun, X.; Liu, H.; Li, Y.; Hao, J. CA-Markov model-based identification of impacts of land use on landscape pattern. *J. Ecol. Rural Environ.* **2009**, *25*, 1–7+31.
14. Hamad, R.; Balzter, H.; Kolo, K. Predicting land use/land cover changes using a CA-Markov model under two different scenarios. *Sustainability* **2018**, *10*, 3421. [CrossRef]
15. Lin, J.; Chen, Q. Analyzing and Simulating the Influence of a Water Conveyance Project on Land Use Conditions in the Tarim River Region. *Land* **2023**, *12*, 2073. [CrossRef]
16. Cong, W.; Sun, X.; Luan, X. Simulation of land use change in Nansihu Lake Basin based on the CLUE-S model. *J. Qu Fu Normal Univ.* **2021**, *47*, 106–112.
17. Gu, H.; Ma, T.; Qian, F.; Cai, Y. Simulation of county land use scenario and carbon emission effect analysis based on CLUE-S model. *J. Agric. Eng.* **2022**, *38*, 288–296. [CrossRef]
18. Liu, J.; Lin, Y.; Zhao, J. County land use change simulation and expansion analysis based on FLUS model. *J. Urban Geo. Investig. Sur.* **2022**, *2*, 16–21.
19. Tang, J.; Hu, X.; Wei, B.; Luo, Z.; Zhao, S.; Wang, Y. Land use change prediction and hydrological response assessment of watershed based on FLUS model. *J. Yangtze River Sci. Res. Inst.* **2022**, *39*, 63–69. [CrossRef]
20. Li, L.; Song, Y.; Wei, X.; Dong, J. Exploring the Impacts of Urban Growth on Carbon Storage under Integrated Spatial Regulation: A Case Study of Wuhan, China. *Ecol. Indic.* **2020**, *111*, 106064. [CrossRef]
21. Liang, Y.; Hashimoto, S.; Liu, L. Integrated Assessment of Land-Use/Land-Cover Dynamics on Carbon Storage Services in the Loess Plateau of China from 1995 to 2050. *Ecol. Indic.* **2021**, *120*, 106939. [CrossRef]
22. Qiu, Z.; Feng, Z.; Song, Y.; Li, M.; Zhang, P. Carbon Sequestration Potential of Forest Vegetation in China from 2003 to 2050: Predicting Forest Vegetation Growth Based on Climate and the Environment. *J. Clean. Prod.* **2020**, *252*, 119715. [CrossRef]
23. Speak, A.; Escobedo, F.J.; Russo, A.; Zerbe, S. Total Urban Tree Carbon Storage and Waste Management Emissions Estimated Using a Combination of LiDAR, Field Measurements and an End-of-Life Wood Approach. *J. Clean. Prod.* **2020**, *256*, 120420. [CrossRef]
24. Mallick, J.; Almesfer, M.K.; Alsubih, M.; Ahmed, M.; Ben Kahla, N. Estimating Carbon Stocks and Sequestration with their Valuation under a Changing Land Use Scenario: A Multi-Temporal Research in Abha City, Saudi Arabia. *Front. Ecol. Environ.* **2022**, *10*, 905799. [CrossRef]
25. Zhu, X.; Li, J.; Cheng, H.; Zheng, L.; Huang, W.; Yan, Y.; Liu, H.; Yang, X. Assessing the Impacts of Ecological Governance on Carbon Storage in an Urban Coal Mining Subsidence Area. *Ecol. Inform.* **2022**, *72*, 101901. [CrossRef]
26. Yang, J.; Xie, B.; Zhang, D. Spat-temporal evolution of carbon stocks in the Yellow River Basin basedon InVEST and CA-Markov models. Chin. *J. Eco-Agric.* **2021**, *29*, 1018–1029. [CrossRef]
27. Wei, Y.; Zhou, W.; Yu, D.; Zhou, L.; Fang, X.; Zhao, W.; Bao, Y.; Meng, Y.; Dai, L. Carbon storage of forest vegetation under the Natural Forest Protection Program in Northeast China. *J. Ecol.* **2014**, *34*, 5696–5705. [CrossRef]
28. Liu, J.; Kuang, W.; Zhang, Z.; Xu, X.; Qin, Y.; Ning, J.; Zhou, W.; Zhang, S.; Li, R.; Yan, C.; et al. Spatiotemporal Characteristics, Patterns, and Causes of Land-Use Changes in China since the Late 1980s. *J. Geogr. Sci.* **2014**, *24*, 195–210. [CrossRef]
29. Li, M.; Zhang, J.; Gao, H.; Ji, G.; Li, G.; Li, L.; Li, Q. Spatiotemporal Variation Characteristics of Ecosystem Carbon Storage in Henan Province and Future Multi-Scenario Simulation Prediction. *Land* **2024**, *13*, 185. [CrossRef]
30. He, Y.; Ma, J.; Zhang, C.; Yang, H. Spat-Temporal Evolution and Prediction of Carbon Storage in Guilin Based on FLUS and InVEST Models. *Remote Sens.* **2023**, *15*, 1445. [CrossRef]
31. Guo, Y.; Ren, H. Remote Sensing Monitoring of Maize and Paddy Rice Planting Area Using GF-6 WFV Red Edge Features. *J. Comput. Electron. Agric.* **2023**, *207*, 107714. [CrossRef]
32. Zhao, W.; Liu, Y.; Guo, D.; Zou, D. Development Application of Rural Domestic Sewage Treatment Project in Cold Areas of Northeast China: Opportunities and Challenges. *J. Water Process Engin.* **2023**, *56*, 104326. [CrossRef]
33. Jiang, Y.; Ouyang, B.; Yan, Z. The Response of Carbon Storage to Multi-Objective Land Use/Cover Spatial Optimization and Vulnerability Assessment. *Sustainability* **2024**, *16*, 2235. [CrossRef]
34. Zheng, H.; Zheng, H. Assessment and Prediction of Carbon Storage Based on Land Use/Land Cover Dynamics in the Coastal Area of Shandong Province. *Ecol. Indic.* **2023**, *153*, 110474. [CrossRef]
35. Cai, W.; Peng, W. Exploring Spatiotemporal Variation of Carbon Storage Driven by Land Use Policy in the Yangtze River Delta Region. *Land* **2021**, *10*, 1120. [CrossRef]
36. Xiang, S.; Wang, Y.; Deng, H.; Yang, C.; Wang, Z.; Gao, M. Response and Multi-Scenario Prediction of Carbon Storage to Land Use/Cover Change in the Main Urban Area of Chongqing, China. *Ecol. Indic.* **2022**, *142*, 109205. [CrossRef]
37. Zhu, Z.; Mei, Z.; Li, S.; Ren, G.; Feng, Y. Evaluation of Ecological Carrying Capacity and Identification of Its Influencing Factors Based on Remote Sensing and Geographic Information System: A Case Study of the Yellow River Basin in Shaanxi. *Land* **2022**, *11*, 1080. [CrossRef]
38. Xu, C.; Zhang, Q.; Yu, Q.; Wang, J.; Wang, F.; Qiu, S.; Ai, M.; Zhao, J. Effects of Land Use/Cover Change on Carbon Storage between 2000 and 2040 in the Yellow River Basin, China. *Ecol. Indic.* **2023**, *151*, 110345. [CrossRef]
39. Guo, H.; He, S.; Jing, H.; Yan, G.; Li, H. Evaluation of the Impacts of Change in Land Use/Cover on Carbon Storage in Multiple Scenarios in the Taihang Mountains, China. *Sustainability* **2023**, *15*, 14244. [CrossRef]
40. Li, H. Evaluation of Ecological Effect of Returning Farmland to Forest Project in Liaoning Province Based on Remote Sensing and InVEST Model. Master's Thesis, Jilin University, Changchun, China, 2019.

41. Liu, Q.; Yang, D.; Cao, L.; Anderson, B. Assessment and Prediction of Carbon Storage Based on Land Use/Land Cover Dynamics in the Tropics: A Case Study of Hainan Island, China. *Land* **2022**, *11*, 244. [CrossRef]
42. Wu, X.; Shen, C.; Shi, L.; Wan, Y.; Ding, J.; Wen, Q. Spatio-Temporal Evolution Characteristics and Simulation Prediction of Carbon Storage: A Case Study in Sanjiangyuan Area, China. *Ecol. Inform.* **2024**, *80*, 102485. [CrossRef]
43. Zhang, Y.; Liao, X.; Sun, D. A Coupled InVEST-PLUS Model for the Spatiotemporal Evolution of Ecosystem Carbon Storage and Multi-Scenario Prediction Analysis. *Land* **2024**, *13*, 509. [CrossRef]
44. Zhao, Y.; Liu, S.; Liu, H.; Dong, Y.; Wang, F. Nature's Contributions to People Responding to Landscape Stability in a Typical Karst Region, Southwest China. *Appl. Geogr.* **2024**, *163*, 103175. [CrossRef]
45. Ma, Z.; Duan, X.; Wang, L.; Wang, Y.; Kang, J.; Yun, R. A Scenario Simulation Study on the Impact of Urban Expansion on Terrestrial Carbon Storage in the Yangtze River Delta, China. *Land* **2023**, *12*, 297. [CrossRef]
46. Wang, Y.; Li, M.; Jin, G. Exploring the Optimization of Spatial Patterns for Carbon Sequestration Services Based on Multi-Scenario Land Use/Cover Changes in the Changchun-Jilin-Tumen Region, China. *J. Clean. Prod.* **2024**, *438*, 140788. [CrossRef]
47. Clerici, N.; Cote-Navarro, F.; Escobedo, F.J.; Rubiano, K.; Villegas, J.C. Spat-Temporal and Cumulative Effects of Land Use-Land Cover and Climate Change on Two Ecosystem Services in the Colombian Andes. *Sci. Total Environ.* **2019**, *685*, 1181–1192. [CrossRef]
48. Zhang, Y.; Naerkezi, N.; Zhang, Y.; Wang, B. Multi-Scenario Land Use/Cover Change and Its Impact on Carbon Storage Based on the Coupled GMOP-PLUS-InVEST Model in the Hexi Corridor, China. *Sustainability* **2024**, *16*, 1402. [CrossRef]
49. Fan, L.; Cai, T.; Wen, Q.; Han, J.; Wang, S.; Wang, J.; Yin, C. Scenario Simulation of Land Use Change and Carbon Storage Response in Henan Province, China: 1990–2050. *Ecol. Indic.* **2023**, *154*, 110660. [CrossRef]
50. Li, P.; Chen, J.; Li, Y.; Wu, W. Using the InVEST-PLUS Model to Predict and Analyze the Pattern of Ecosystem Carbon Storage in Liaoning Province, China. *Remote Sens.* **2023**, *15*, 4050. [CrossRef]
51. Geng, X.; Li, W.; Min, C. Analysis of the evolution characteristics of carbon reserves in Chengdu based on land use change. *J. Environ. Impact Rev.* **2023**, *45*, 104–112. [CrossRef]
52. Chen, Y.; Luo, G.; Ye, H.; Wang, Y.; Huang, X.; Zhang, Q.; Cai, P. Impact of land use/cover change in Central Asia from 1975 to 2005. *J. Nat. Resour.* **2015**, *30*, 397–408. [CrossRef]
53. Heng, Z.; Ge, L.; Zi, Y. Ecosystem service assessment and multi-scenario prediction in Liaoning Province from 2000 to 2020. *J. Environ Sci.* **2024**, *45*, 4137–4151. [CrossRef]
54. Zhang, C.; Xiang, Y.; Fang, T.; Chen, Y.; Wang, S. Spatial and temporal change and prediction of carbon reserves in Taiyuan ecosystem under the influence of LUCC. *J. Saf. Environ. Engin.* **2022**, *29*, 248–258. [CrossRef]
55. Nie, X.; Lu, B.; Chen, Z.; Yang, Y.; Chen, S.; Chen, Z.; Wang, H. Increase or Decrease? Integrating the CLUMondo and InVEST Models to Assess the Impact of the Implementation of the Major Function Oriented Zone Planning on Carbon Storage. *Ecol. Indic.* **2020**, *118*, 106708. [CrossRef]
56. Zhu, L.Y.; Hu, K.; Sun, S.; Liu, Y.; Liang, J.X. Research on the spatiotemporal variation of carbon storage in the coastal zone of Liaoning Province based on InVEST model. *J. Geosci.* **2022**, *36*, 96–104.
57. Lv, J. Spatial distribution characteristics of soil conservation function in the ecosystem of Liaoning Province. *J. Environ. Prot. Circ. Econ.* **2019**, *39*, 38–41.
58. Lee, J.-G.; Lee, D.-H.; Jung, J.-Y.; Lee, S.-G.; Han, S.H.; Kim, S.; Kim, H.-J. The Effects of Stand Density Control on Carbon Cycle in *Chamaecyparis obtusa* (Siebold and Zucc.) Endl. *Forests* **2023**, *14*, 217. [CrossRef]
59. Yuan, H.; Zhang, Z.; Feng, D.; Rong, X.; Zhang, S.; Yang, S. Assessment of the Impact of Land Use/Land Cover Change on Carbon Storage in Chengdu, China, in the Context of Carbon Peaking and Carbon Neutrality, 2000–2030. *Environ. Dev. Sustain.* **2024**, 1–24. [CrossRef]